

## 1-Introduction

Ni-Zn polycrystalline ferrites (NZF) are low-cost materials that are attractive for microwave device applications, with spinel structure has a promising potential as high performance microwave devices owing to its high resistivity, mechanical hardness, high Curie temperature, chemical stability, and soft magnetic properties at high frequency. It is well known that the intrinsic parameters of these ferrites depend on the composition. Properties of ferrites are known to be sensitive to the processing technique [A. Verma 2000]. Soft ferrites such as, Ni-Zn are well known ferrites covering wide-ranging applications. These ferrites have been widely used in electronic applications such as transformers, choke coils, noise filters, and recording heads. By introduction of a relatively small amount of foreign ions, an important modification of both structure and magnetic properties can be obtained [Rezlescu E, Rezlescu N 1992, 1993]. The electrical resistivity of ferrite at room temperature depending upon the chemical composition which lies between about  $10^3$  Ohm-cm and  $10^8$  Ohm-cm. Low resistivity due to hopping of bonding electrons are caused by the simultaneous presence of  $Fe^{3+}$  and  $Fe^{2+}$  ions on crystallographically equivalent lattice sites. The resistivities of several ferrites are found to depend sensitively on firing conditions, temperature and atmosphere and on the ions that substitute  $Fe^{3+}$  /  $Fe^{2+}$  ions. Ferrites with the properties of large resistivity, low core loss and low eddy currents are being used for a variety of high frequency applications. Substitution of divalent ion in to the spinel structure has been reported to lead to structural distortion. That induces strains in the material and to affect the electrical and magnetic properties significantly. There are several synthesis techniques such as solid-state reaction method, hydro-thermal method, precipitation/co-precipitation method and sol-gel auto-combustion method for the preparation of nanoferrites. Among these processes, co-precipitation has lately shown to be a very promising technique for the preparation of ultrafine ferrite particles of controlled size and morphology with a number of applications. [W.Y. Huang, 2005, A. Verma (1999)]

Most of the work on the preparation of ferrite through hydrothermal processing has been carried out using (NaOH) and the major impurity present [M.T. Johnson (1992)].

*The aim of this work was to evaluate the influence of the various Cadmium ions on the ceramic parameters of a (NiZn) ferrite. The dielectric and magnetic properties.*

## 2. Experimental

The powders of Ni- ferrites, Zn- ferrites & Cd- ferrites were prepared using Co-precipitation auto-combustion method from  $FeCl_3$ ,  $Ni(NO_3)_2$ ,  $ZnC_4H_6O_4 \cdot 2H_2O$  &  $CdCO_3$  as starting material. Each one dissolved in (400) ml Distil water, Ferrites have been synthesized using aqueous ammonia to avoid incorporation of sodium. Control of synthesis parameters has resulted in the production of ferrite particles, having a meta stable cation distribution as revealed from micro structural and magnetic studies. The pH of the solution was adjusted to 7-9 using ammonia solution. The solution was uniformly heated at  $100^\circ C$  with constant stirring to transform it into a gel and then filtered gel was obtained by dehydration process. The dried gel was combusted with the evolution of large amount of gases and it resulted in the formation of loose powder [M.T. Johnson (1992) M.C. Dimri, (2006)]. The prepared powder was then calcined at  $800^\circ C$ . Three type of ferrite were synthesized which are of Ni- ferrites, Zn- ferrites & Cd- ferrites to formed final production with composition  $(Ni Zn)_x Cd_{1-x} Fe_2O_4$   $x=(0.7, 0.4, 0.2, 0.0)$  by mixing every one with properly construction of x- value, then it was pressed (5 tons) as rings ( $R_n$ ) and (3 tons/ $cm^2$ ) as pelt ( $D_n$ ). the temperature of final sintering in this case was kept at  $1100^\circ C$ . The pellet samples were well polished to remove any roughness and the two surfaces of each pellet were coated with silver paste as contact material for electrical and dielectric measurements. Using L.C.R type (micro test 6379), dielectric measurement as a function of frequency in the range (20 Hz–3 MHz) at room temperature. The real part of dielectric constant was calculated using the formula

$$\epsilon_r = \frac{C d}{\epsilon^0 A} \quad (1)$$

Where  $C$  is the capacitance measured of the pellet in pF,  $d$  the thickness of the pellet,  $A$  the cross-sectional Area of the flat surface of the pellet and  $\epsilon^0$  the constant of permittivity for free space.

The imaginary dielectric constant ( $\epsilon_i$ ) and loses factor ( $\tan\delta$ ) was measured over the same frequency range (20 Hz-3 MHz) to calculate the imaginary part of dielectric constant using the formula

$$\tan\delta = \frac{\epsilon_i}{\epsilon_r} \quad (2)$$

Also the magnetic properties was measured by the same equipment, (initial permeability  $\mu$ ) was calculate after measuring the inductors ( $L$ ) then by using the formula (MMPA 1998)

$$\mu_i = \frac{L}{L^0} \quad (3)$$

$$L^0 = 4.6 N^2 d \log(r_{out}/r_{in}) = L_0$$

where  $r_{in}$  is the inner radius and  $r_{out}$  is the outer radius,  $d$  is thickness of samples,  $L$  = the inductors of sample,  $N$  = the numbers of turns

### 3. Results and discussion:

#### 3-1. XRD discussion

The phase identification and lattice constant determination were performed by x-ray diffraction pattern (XRD). Typical XRD pattern of ferrites sample is shown in Fig. (1), (2), (3), and (4).

All the samples show good crystallization, with well-defined diffraction lines. The structure can be indexed as a single-phase cubic spinel structure. It is obvious that the characteristic peaks for spinel ferrites appear in the samples as the main crystalline phase. The peaks (2 2 0), (3 1 1), (2 2 2), (4 0 0), (4 2 2), (5 1 1) and (4 4 0) correspond to spinel structure, lattice parameter was determined (a) & crystal Density was Calculated from equ.

Where  $Z$  is the number molecules per unit cell of spinel lattice,  $M$  is the molecular weight of the samples,  $N$  is the Avogadro's number and  $a$  is the lattice parameter.

Then porosity  $p\%$  will be calculated from equ.

$$P = 1 - \frac{D_B}{D_x} \times 100 \%$$

when  $D_B$  was bulk density,  $D_x$ : was crystal density

the lattice parameter ' $a$ ' as a function of  $Cd^{2+}$  content  $x$  is depicted in table (1). It is noticed that the lattice parameter increases with the cadmium content in the lattice. This variation can be explained on the basis of an ionic size difference of the component ions. The  $Cd^{2+}$  ions have a larger ionic radius (0.97 Å) than the  $Zn^{2+}$ ,  $Ni^{2+}$  (0.65 Å) ions [D.N. Bhosale (1999)].

The  $Cd^{2+}$  ions successively replace the  $Ni^{2+}$  &  $Zn^{2+}$  ions in B-site. The unit cell expands to accommodate the larger ions. Thus addition of  $Cd^{2+}$  at the expense of the  $Ni^{2+}$  &  $Zn^{2+}$  in the ferrite is expected to increase the lattice parameter.

**3-2 Real & imaginary part of dielectric constant ( $\epsilon_r, \epsilon_i$ ):** The dielectric behavior in ferrite can be explained based on the assumption that the mechanism of dielectric polarization is similar to that of conduction. Many scientists have established a strong correlation between the conduction mechanism and dielectric constant of ferrite [K. Iwachi, (1971), C. Jain (1982)]. It has been explained that dielectric behavior based on a number of available  $Fe^{2+}$  ions. The

electronic change such as  $Fe^{2+} \leftrightarrow Fe^{3+}$  results in a local displacement of electron, which determines the polarization and thus the dielectric constant of ferrite. It has been observed that from Fig.(5) which shows the variation of the ( $\epsilon_r$ ) behavior with increasing frequency then Fig (6) gave us the magnitude of ( $\epsilon_r$ ) with change X-value by using some magnitude of frequency, Fig.(7) which shows the dielectric dispersion curves can be explained on the basis of Koop's two layer model and Maxwell- Wagner polarization theory. To interpret the frequency response of dielectric constant in ferrite and dielectric materials, Koop's [C. G. Koops (1951).] suggests a theory in which relatively good conduction grains and isolating grain boundary layers of ferrite material can be represented with the behavior of an inhomogeneous dielectric structure. An assembly of space charge carriers in the inhomogeneous dielectric structure, is discussed by Maxwell and Wagner [J. C. Maxwell (1982)]. Since an assembly of space charge carrier in the inhomogeneous dielectric structure described requires finite time to line up their axis parallel to an alternating electric field, the dielectric constant naturally decreases, if the frequency of reversal field increases.

$$\tau = \frac{1}{\omega} \quad , \quad \omega = 2\pi f_{\max}$$

$$\therefore \tau = \frac{1}{2\pi f_{\max}} \quad \text{where } \tau: \text{ the relaxation time } \omega: \text{ angular velocity}$$

### 3-3A.C Conductivity :

Figs (10) shows the variation of a.c conductivity behavior with frequency for  $(NiZn)_x Cd_{1-x} Fe_2O_4$  systems at room temperature in the range of about (20 Hz-3MHz), with different x-value while Fig(11) shows the magnitude variation of a.c conductivity with same parameters. According to Maxwell- Wagner theory, two layers forming dielectric structure. The first layer consists of ferrite grains of fairly well conducting (ferrous ions), which is separated by a thin layer of poorly conducting substances, which forms the grain boundary. These grain boundaries are more active at lower frequencies; hence, the hopping frequency of electron between  $Fe^{3+}$  and  $Fe^{2+}$  ions is less at lower frequencies. As the frequency of the applied field increases the conductive grains become more active by promoting the hopping of electron between  $Fe^{2+}$  and  $Fe^{3+}$  ions, thereby increasing the hopping frequency. Thus, we observe a slight increase in conductivity with frequency.

### 3-4 Vibrating Sample Magnetometer (VSM)

Figure 12 shows the magnetic hysteresis loops of  $(NiZn)_x Cd_{1-x} Fe_2O_4$  samples taken by vibrating sample magnetometer at room temperature showing typical magnetic behavior having a non-zero coercivity and remanance. The value of magnetic saturation, coercivity and remanance that concluded was shown at table No.(2). Low area hysteresis curve shows that the material formed is of soft magnetic material. The hysteresis loops of all ferrite samples tend towards paramagnetic behavior with increase of the cadmium content in the ferrites then it will be as super paramagnetic behavior at  $X=0.0$  when the synthesis will be  $CdFe_2O_4$ . The  $Cd^{2+}$  &  $Zn^{2+}$  ion strongly occupies the tetrahedral A-site [S.A. Patil (1998), O.M. Hemedat, (2001).] while  $Ni^{2+}$  the octahedral B-site [G.K. Joshi, (1988)] and  $Fe^{3+}$  ions occupy both tetrahedral and octahedral sites. The addition of cadmium a nonmagnetic divalent metal ion ( $Cd^{2+}$  ion) content in ferrites reduces the amount of  $Ni^{2+}$  ions and increases the amount of  $Fe^{3+}$  ions in ferrites on B-site was responsible for the super paramagnetic behavior. The occupancy of  $Cd^{2+}$  ion at tetrahedral site (A-site) successively replaces  $Fe^{3+}$  ions from A-site and transfers equal amount of  $Fe^{3+}$  ions to B-site. The decrease of magnetic moment of tetrahedral site with increase of Cd ion content is due to the decrease of  $Fe^{3+}$  ions content on A-site. The addition of  $Cd^{2+}$  ion in the ferrites decreases the amount of  $Ni^{2+}$  ion and increases the amount of  $Fe^{3+}$  ions on B-site, increases the magnetic moment of octahedral site (B-site).

In this work an effort was made to synthesize ferrite powder by a very simple process of co-precipitation which gained a reasonably incredible success, resulting good magnetic properties as shown by hysteresis curve.

### 3-5 Magnetic Permeability ( $\mu_i$ )

Figs.13 shows variation the behavior of real part of permeability as a function of frequency. As its clear from figs.13 permeability decrease with increased frequency, that's due to the relation between magnetic inductance and frequency which act as the major caused in this decrease, whereas increasing frequency caused dipoles oscillations more aligned, that's cause inverse current, so that the inductance current decrease abruptly at low frequency, then changes become very small as its clear seem behavior for all samples.

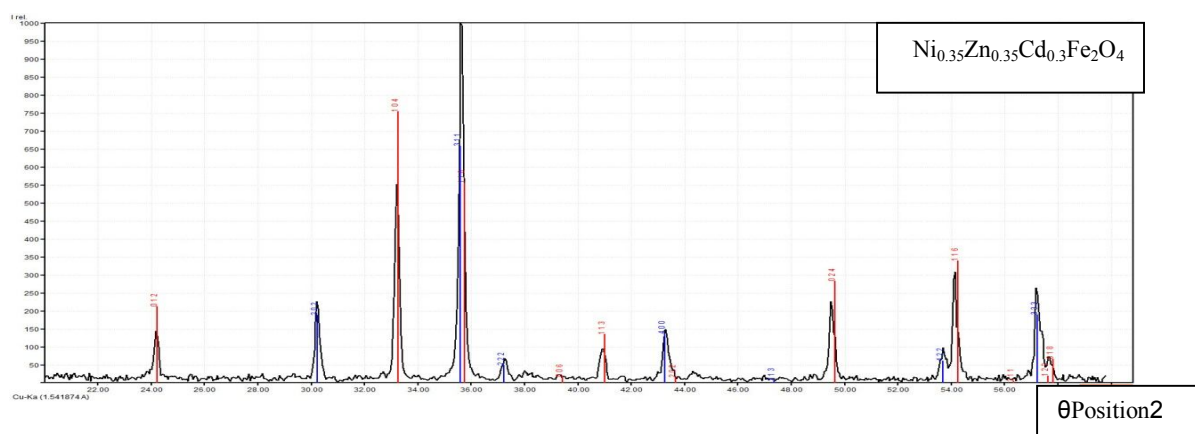
while fig.14 shows variation the magnitude of magnetic permeability with frequency & X-value change for  $(\text{NiZn})_x\text{Cd}_{1-x}\text{Fe}_2\text{O}_4$  system.

### 4-CONCLUSIONS:

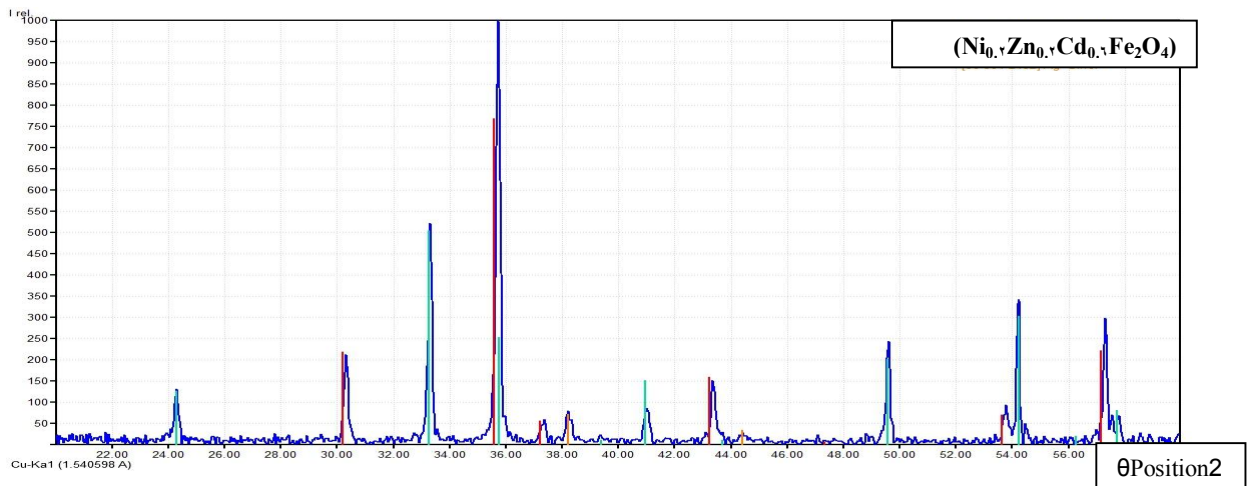
1. decreasing dielectric constant & dielectric losses factor ( $\epsilon_r, \epsilon_i$ ) with increasing frequency, the sample D4 ( $\text{Ni}_{0.1}\text{Zn}_{0.1}\text{Cd}_{0.8}\text{Fe}_2\text{O}$ ) was the highest magnitude of these parameter.
2. increasing the A.c conductivity  $\sigma_{(a.c)}$  with increasing the frequency
3. the hysteresis loop for the All sample has small area As soft ferrite except ( $\text{CdFe}_2\text{O}$ ).
4. decreasing the magnetic Permeability ( $\mu_i$ ) with increasing frequency.

Table (1) X-value for sample No. with some Parameter calculated by XRD test

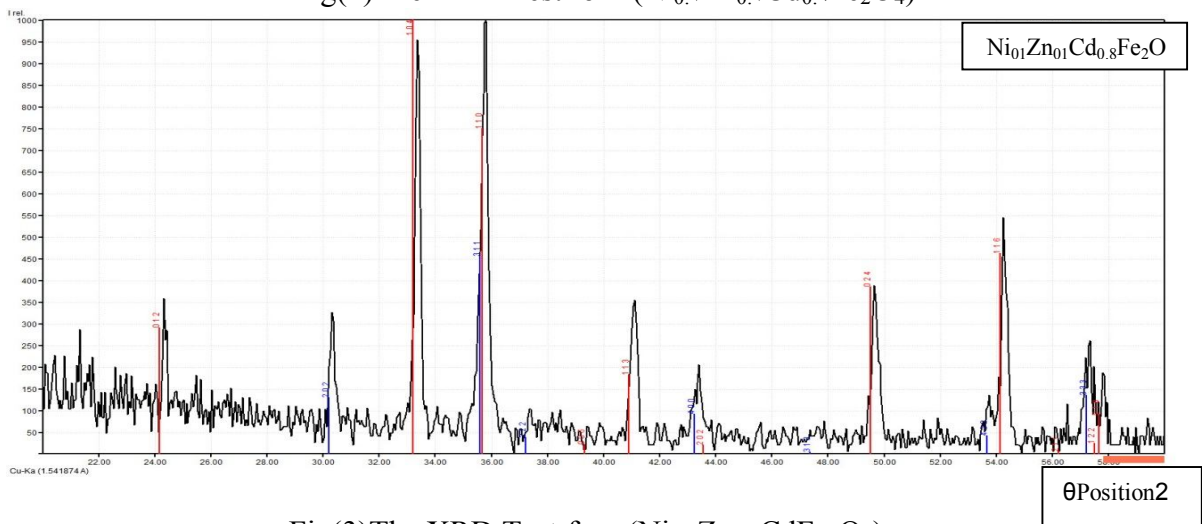
Sample No.	X-Value equivalent to $\text{Cd}^{2+}$ ion content	Lattice Parameter (a) $\text{\AA}$	Crystal density $D_x(\text{g}/\text{Cm}^3)$	Bulk density $D_B(\text{g}/\text{Cm}^3)$	Porosity P%
D2	0,7	1,70	0,03	3.77	22%
D3	0,4	1,72	0,322	4.2	20%
D4	0,2	1,74	0,032	4.33	18%
D5	0,0	1,77	0,66	4.72	17%



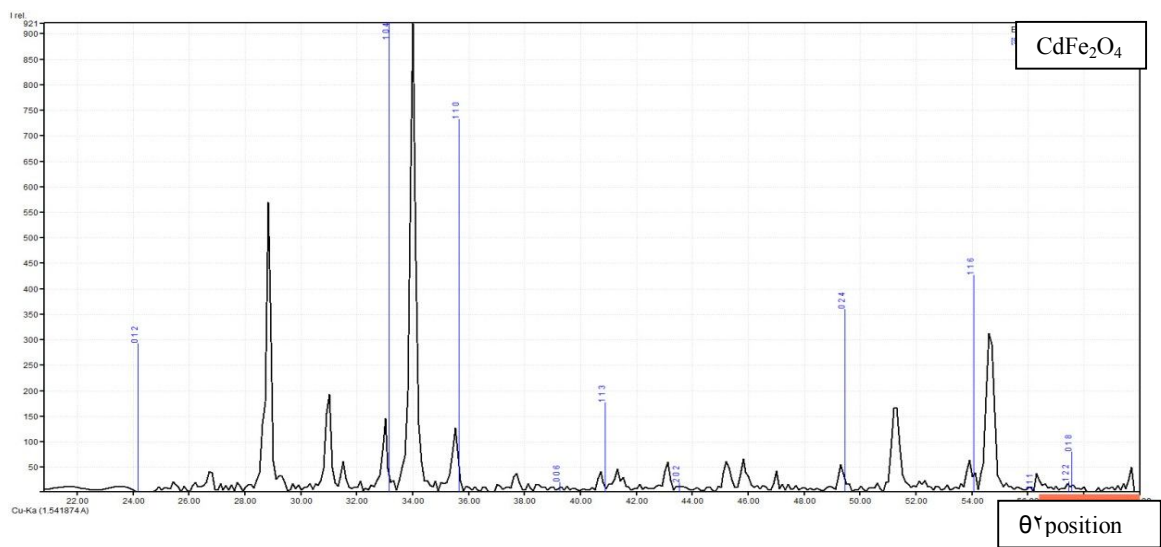
Fig(1) The XRD Test for  $(\text{Ni}_{0.35}\text{Zn}_{0.35}\text{Cd}_{0.3}\text{Fe}_2\text{O}_4)$



Fig(2)The XRD Test for  $(Ni_{0.7}Zn_{0.7}Cd_{0.7}Fe_2O_4)$

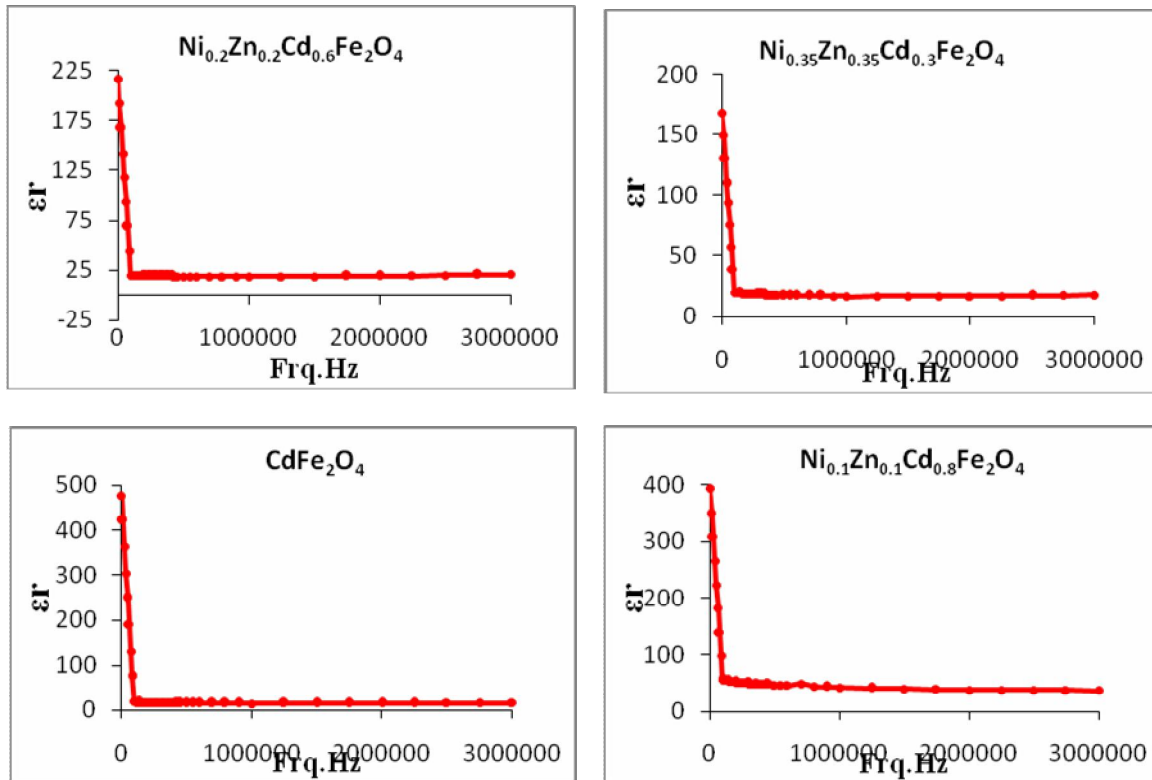


Fig(3)The XRD Test for  $(Ni_{0.1}Zn_{0.1}Cd_{0.8}Fe_2O_4)$

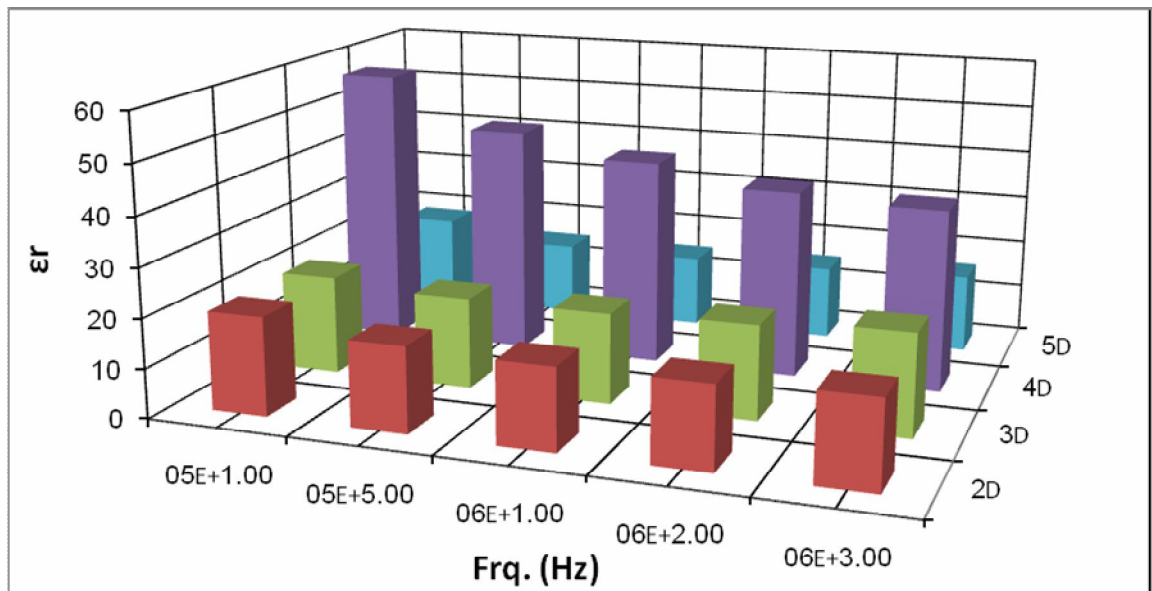


Fig(4)The (XRD)Test for  $CdFe_2O_4$





Fig(5) Variation of dielectric constant behavior with frequency for  $(\text{NiZn})_x \text{Cd}_{1-x} \text{Fe}_2\text{O}_4$  system



Fig(6) Variation magnitude of dielectric constant with frequency & X-value change for  $(\text{NiZn})_x \text{Cd}_{1-x} \text{Fe}_2\text{O}_4$  system

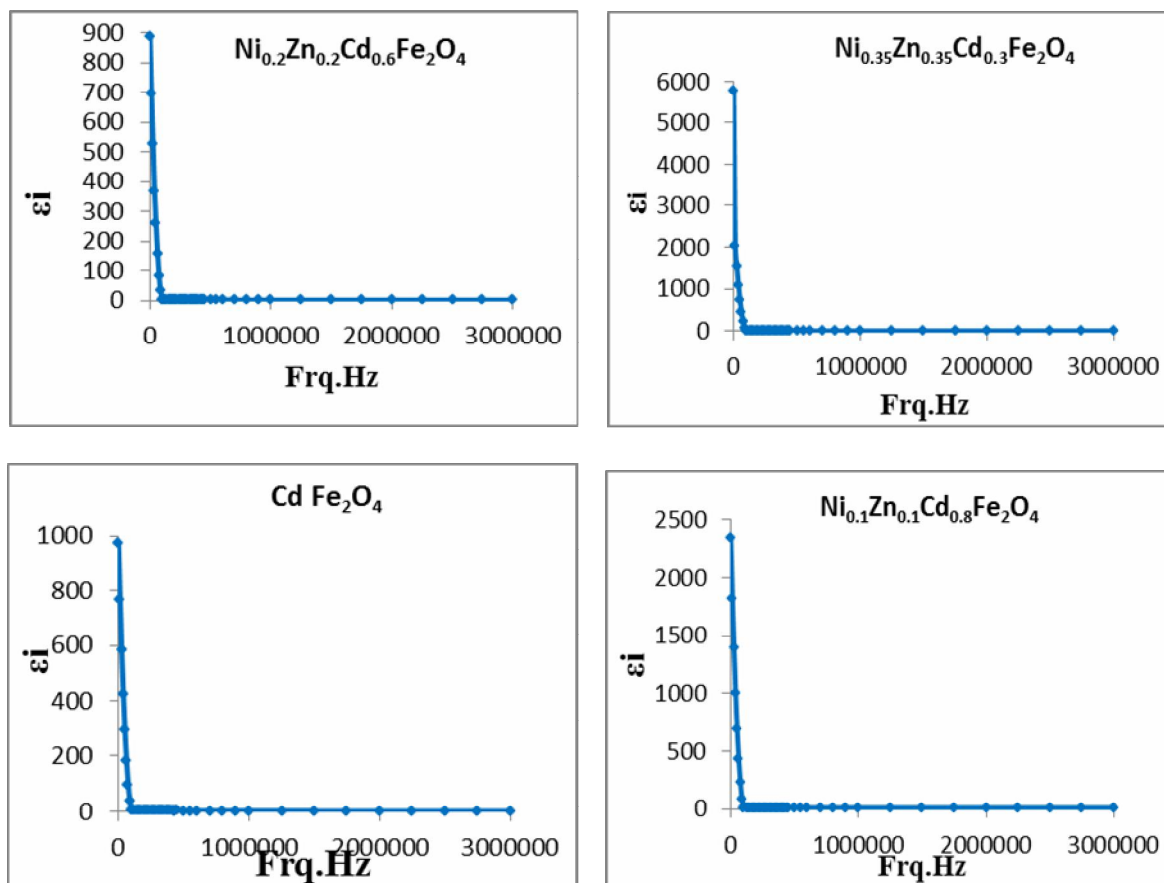
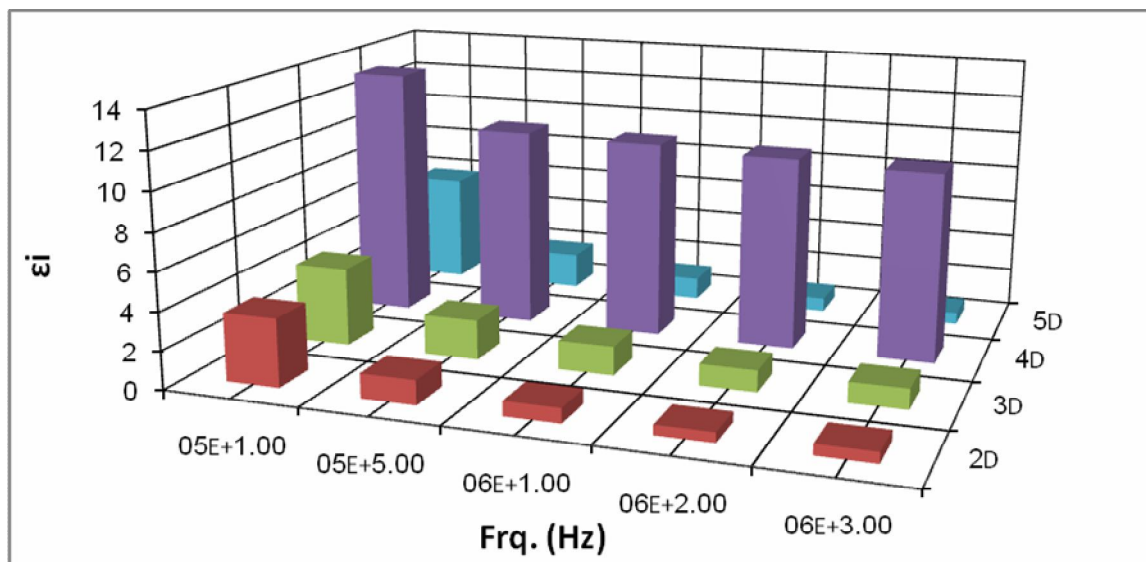


Fig (7)Variation of dielectric loss factor behavior versus frequency for  $(\text{NiZn})_x\text{Cd}_{1-x}\text{Fe}_2\text{O}_4$  system



Fig(8)Variation magnitude of dielectric loss factor with frequency & X-value change for  $(\text{NiZn})_x\text{Cd}_{1-x}\text{Fe}_2\text{O}_4$  system

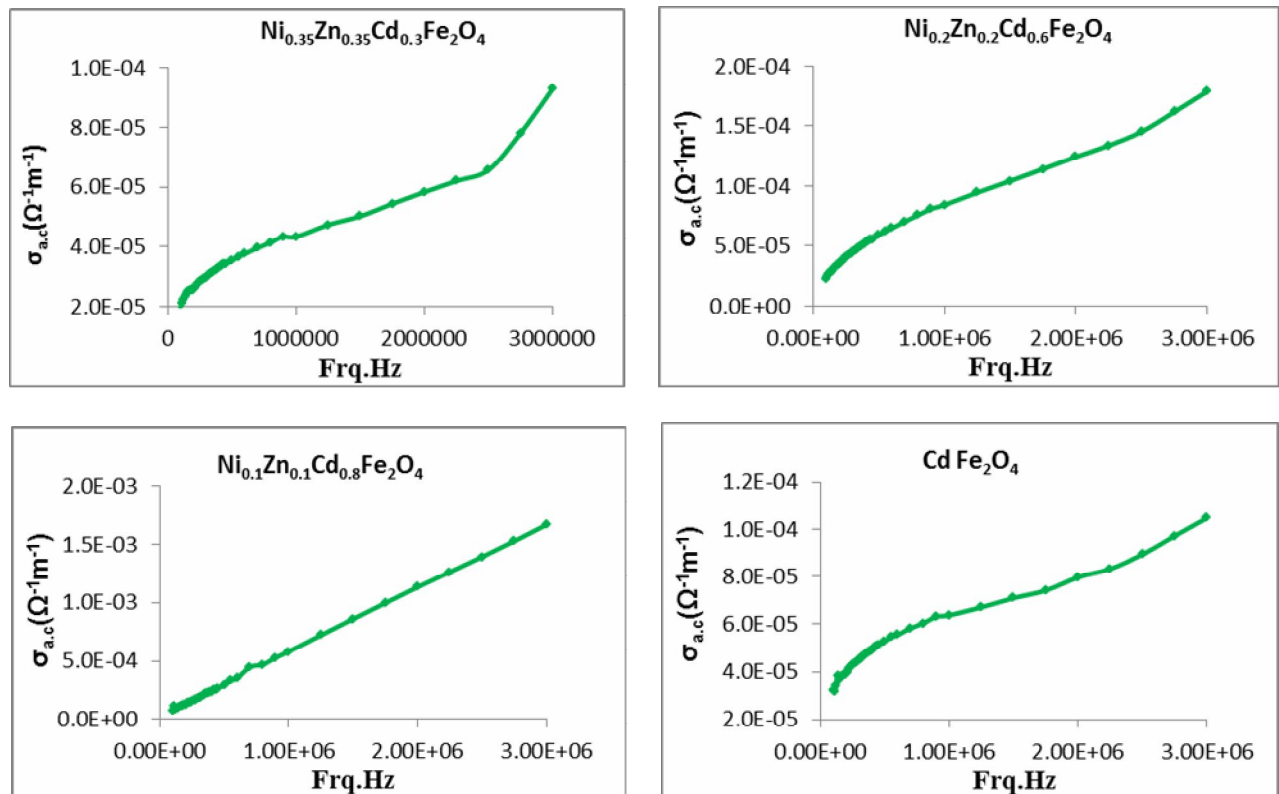
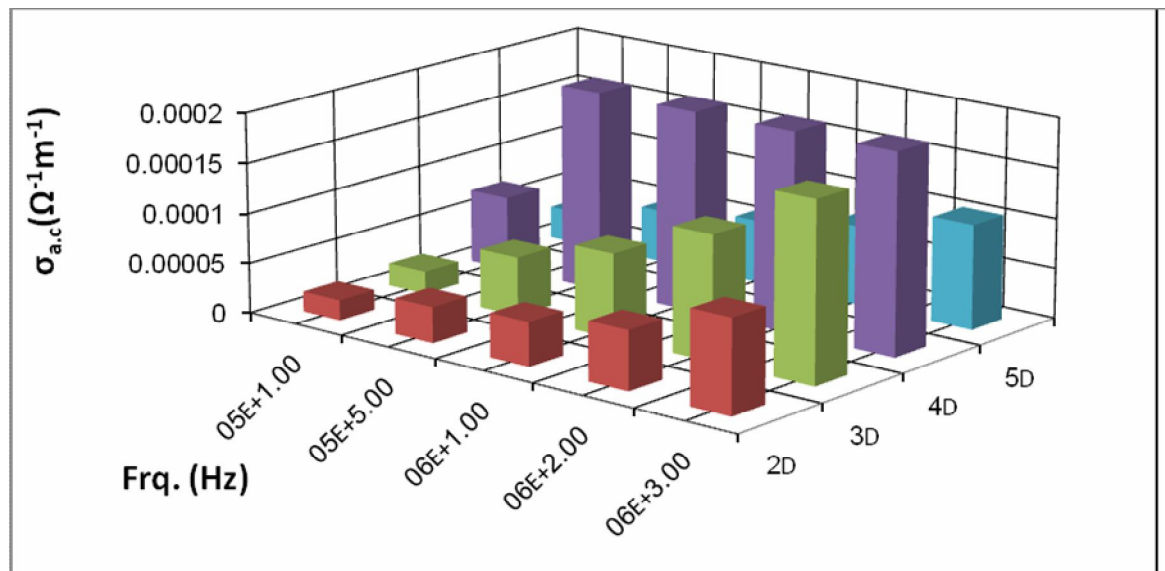


Fig (9) Variation of conductivity behavior with frequency for  $(\text{NiZn})_x\text{Cd}_{1-x}\text{Fe}_2\text{O}_4$  system



Fig(10) Variation magnitude of conductivity with frequency & X-value change for  $(\text{NiZn})_x\text{Cd}_{1-x}\text{Fe}_2\text{O}_4$  system



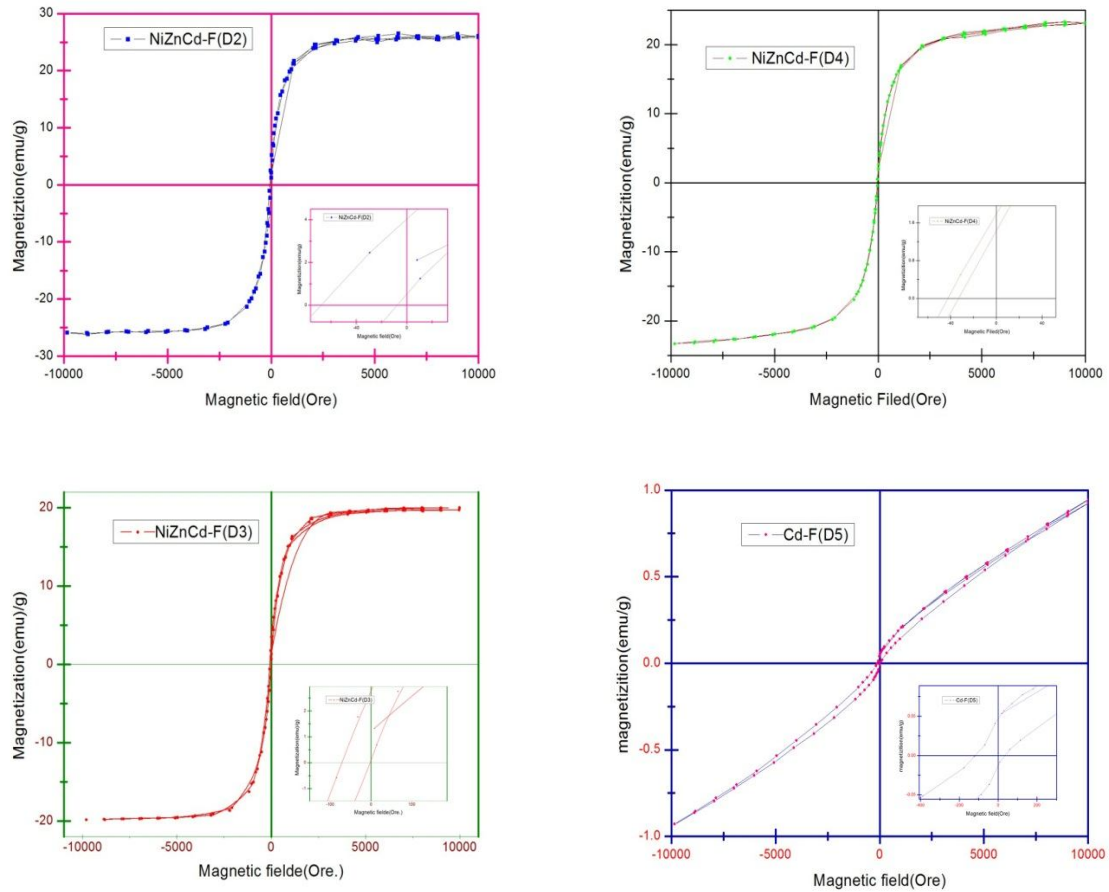


Fig.(11) Variation of hysteresis loop for  $(\text{NiZn})_x\text{Cd}_{1-x}\text{Fe}_2\text{O}_4$  system

Table (2) Show the magnetic parameter which calculated from hysteresis loop diagram

D5 X=0.0	D4 X=0.2	D3 X=0.4	D2 X=0.7	Sample No. parameter
0.945	23.03	20.03	26.1064	$\sigma_s$
0.0469	1.722	2.69	4.05	$\sigma_r$
77	4.74	34.2	30.1	$H_c$

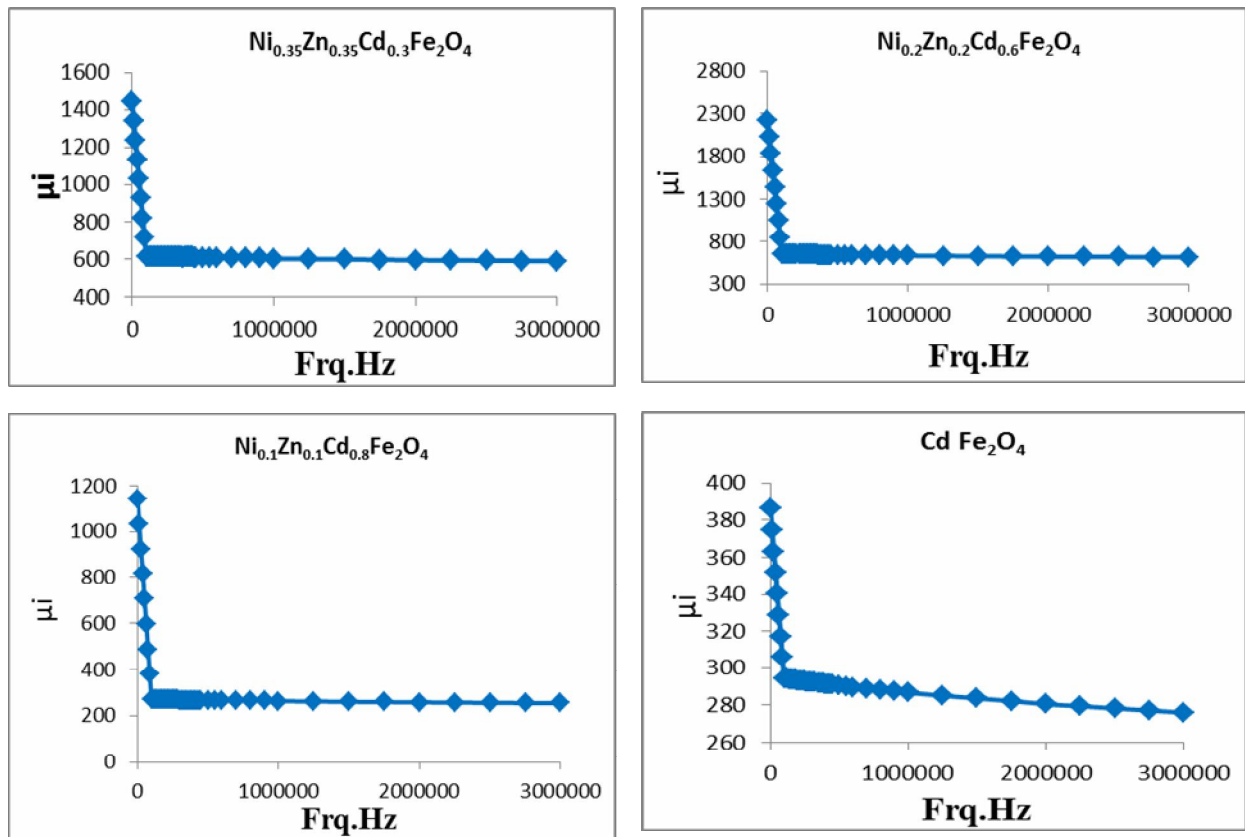
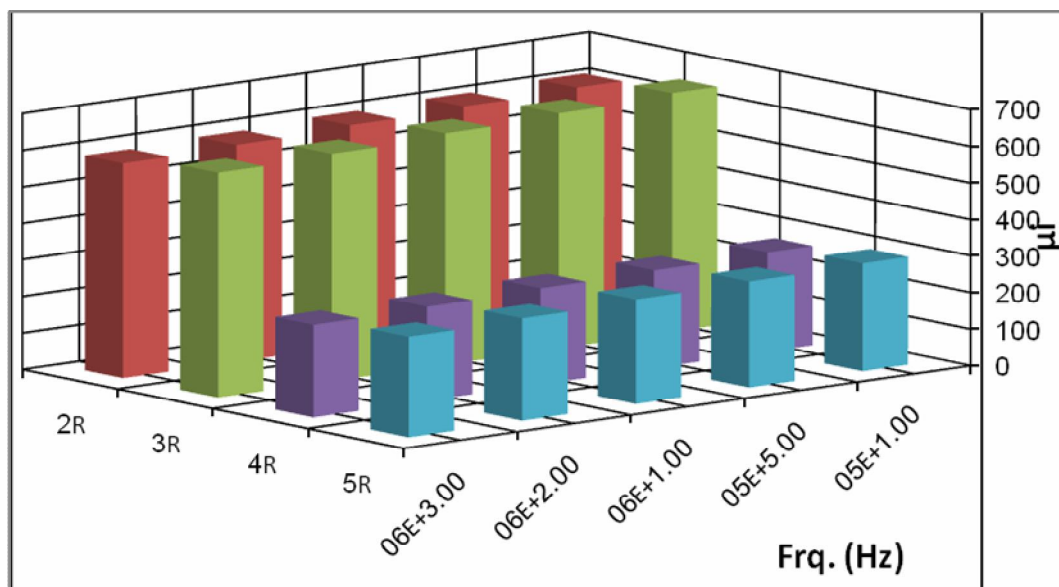


Fig (12) Variation of magnetic permeability behavior with frequency for  $(\text{NiZn})_x \text{Cd}_{1-x} \text{Fe}_2\text{O}_4$  system



Fig(13) Variation magnitude of magnetic permeability with frequency & X-value change for  $(\text{NiZn})_x \text{Cd}_{1-x} \text{Fe}_2\text{O}_4$  system

**REFERENCES:**

A. Verma, T.C. Goel, R.G. Mediratta, Second International Conference on Processing Materials for Properties, The Mineral, Metal & Material Society, 2000, pp. 493–497.

A. Verma, T.C. Goel, R.G. Mendiratta, M.I. Alam, Mater. Sci. Eng. B 60 (1999) 156.

C. G. Koops; physics. Rev., Vol.83, (1951), pp. 121-126.

D.N. Bhosale, S.R. Sawant, S.A. Gangal, R.R. Mahajan, P.P. Bakare, Mater. Sci. Eng. B 65 (1999) 79.

G. C. Jain.; IEEE Trans. Magn. Vol 18, (1982), pp.776-781

G.K. Joshi, A.Y. Khot, S.R. Savant, Solid State Commun. 65 (1988) 1593

J. C. Maxwell; "A Treatise on Electricity and Magnetism", Clarendon Press, Oxford (1982).

K. Iwauchi, J. Appl. Phys., Vol 10, (1971), 1520

M.C.Dimri,A.Verma,S.C.Kashyap,D.C.Dube,O.P.Thakur,C.Prakash,Mater Eng.B133(2006)42

M.T. Johnson, A. Noordermeer, M.M.E. Severin, W.A.M. Meeuwissen, J. Magn. Magn. Sci. Mater. 116 (1992) 16

O.M. Hemeda, M.M. Barakat, J. Magn. Magn. Mater. 223 (2001) 127

]Rezlescu E., Rezlescu N., Craus M.L., Popa P.D., *J.MMM* 117 (1992) 448-454

Rezlescu N., Rezlescu E., Pasnicu C., Craus M.L., *Ceramics International* 19 (1993) 71- 75

S.A. Patil, V.C. Mahajan, A.K. Gatge, S.D. Lotake, Mater. Chem. Phys. 57 (1998) 86

W.Y. Huang, P.Y. Du, W.J. Weng, G.R. Han, J. Mater. Sci. Eng. 23 (2005) 528

Z. Yue, J. Zhou, L. Li, X. Wang, Z. Gui, Mater. Sci. Eng. B 86 (2001) 64